Improvement in SAR Image Classification using Adaptive Stack Filters

María Elena Buemi, Marta Mejail, Julio Jacobo and Juliana Gambini
Universidad de Buenos Aires
Facultad de Ciencias Exactas y Naturales
Departamento de Computación
Ciudad Universitaria, Pabellón I
C1428EGA Buenos Aires – República Argentina
{mebuemi,marta,jacobo,jgambini}@dc.uba.ar

Abstract

Stack filters are a special case of non-linear filters. They have a good performance for filtering images with different types of noise while preserving edges and details. A stack filter decomposes an input image into several binary images according to a set of thresholds. Each binary image is filtered by a Boolean function. The Boolean function that characterizes an adaptive stack filter is optimal and is computed from a pair of images consisting of an ideal noiseless image and its noisy version. In this work the behavior of adaptive stack filters is evaluated for the classification of Synthetic Aperture Radar (SAR) images, which are affected by speckle noise. With this aim it was carried out experiment in which simulated and real images are generated and then filtered with a stack filter trained with one of them. The results of their Maximum Likelihood classification are evaluated and then are compared with the results of classifying the images without previous filtering.

1 Introduction

Stack filters are a special case of non-linear filters. They have a good performance for filtering images with different types of noise while preserving edges and details. Various authors have studied this type of filters and many methods for stack filters design have been developed [4, 5, 9, 11, 15, 16, 17, 20]. These filters decompose the input image by thresholds yielding a binary image for each threshold value. Each binary image is then filtered using a Boolean function evaluated on a sliding window. The resulting image is obtained summing up all the filtered binary images obtained. This Boolean function must be optimal according to de Mean Absolute Error (MAE) criterion and must preserve the so-called stacking property, which will be described in Section 2. The stack filter design method used in this work is based on an algorithm proposed by Yoo *et al.* [21]. In this paper we study the application of this type of filter to Synthetic Aperture Radar (SAR)images as a stage previous to a Maximum Likelihood classification.

SAR images are generated by a coherent illumination system and are affected by the coherent interference of the signal backscatter by the elements on the terrain [8, 14]. This interference causes fluctuations of the detected intensity which varies from pixel to pixel. This effect is called speckle noise. Speckle noise, unlike noise in optical images, is neither Gaussian nor additive; it follows other distributions and is multiplicative. Due to all of this, it is not possible to treat these images using the classical techniques appropiate for optical image processing. Many authors have studied the problem of adapting classical image processing methods to be applied to SAR images using filter-based techniques [10, 12, 18, 19], with some success.

The multiplicative nature of the speckle noise leads us to model the SAR image Z as the product of two independent random images: image X, that represents the backscatter and image Y, that represents the speckle noise. The backscatter is a physical magnitude that depends on the geometry and water content of the surface being imaged, as well as on the angle of incidence, frequency and polarization of the electromagnetic radiation emitted by the radar. Different statistical distributions have been proposed in the literature. In this work we use the Gamma distribution, Γ, for the speckle, the reciprocal of Gamma distribution, Γ^{-1}, for the backscatter, which results in the $\mathcal{G}^0$ distribution for the return [6, 7, 13]. These distributions depend on three parameters: α that is a roughness parameter, γ a scale parameter, and n the equivalent number of looks. In this work, we classify an image into different regions according to their homogeneity degree, which will be refered to section 5. After filtering, the image data have undergone changes in their

statistical distribution functions. These filtered data have a statistical distribution with skewness and kurtosis closer to those of the Gaussian law. Then, we classify the image by using the maximum likelihood method and consider the normal distribution with different parameters for each region. The structure of this paper is as follows: section 2 gives an introduction to stack filters, section 3 describes the filter design method used in this work. In section 4 we summarise the $\mathcal{G}^0$ distribution for SAR images. In section 5 we show the modification undergone by the data after applying the filter, the results of classifying the filtered data and compare these results with the results of applying the Lee and the Frost filter. Finally, in section 6 we present the conclusions.

2 Stack Filters: Definitions and designing

This section is dedicated to a brief synthesis of stack filter definitions and design. For more details on this subject, see [1, 2, 3, 9, 11, 20, 21]. In the first place the necessary definitions are presented to explain this type of filters. The threshold operator is given by $T^m : \{0, 1, \ldots, M\} \rightarrow \{0, 1\}$

$$T^m(x) = \begin{cases} 1 & \text{if} \quad x \geq m \\ 0 & \text{if} \quad x < m \end{cases}, \tag{1}$$

$$X^m = T^m(x). \tag{2}$$

According to this definition, the value of a non-negative integer number $x \in \{0, 1, \ldots, M\}$ can be reconstructed making the summation of its thresholded values between 0 and M. The formula corresponding to this operation is

$$x = \sum_{m=1}^{M} X^m. \tag{3}$$

What follows shows an example of the threshold decomposition of an unidimensional signal.

$$\begin{array}{rl} X = & [2, 1, 4, 5, 3, 2, 4, 3] \\ X^1 = & [1, 1, 1, 1, 1, 1, 1, 1] \\ X^2 = & [1, 0, 1, 1, 1, 1, 1, 1] \\ X^3 = & [0, 0, 1, 1, 1, 0, 1, 1] \\ X^4 = & [0, 0, 1, 1, 0, 0, 1, 0] \\ X^5 = & [0, 0, 0, 1, 0, 0, 0, 0] \end{array}$$

The threshold operator can be extended to bidimensional signals. Let $X = (x_0, \ldots, x_{n-1})$ and $Y = (y_0, \ldots, y_{n-1})$ be binary vectors of length n, then let us define a relation $\leq$ given by

$$X \leq Y \quad \text{if and only if} \quad \forall i,\ x_i \leq y_i. \tag{4}$$

This relation is reflexive, anti-symmetric and transitive, generating therefore a partial ordering on the set of binary vectors of fixed length. A boolean function $f : \{0, 1\}^n \rightarrow \{0, 1\}$, where n is the length of the input vectors, has the stacking property if and only if

$$\forall X, Y \in \{0, 1\}^n,\ X \leq Y \Rightarrow f(X) \leq f(Y). \tag{5}$$

We say that f is a positive boolean function if and only if it can be written by means of an expression that contains only non-complemented input variables. That is,

$$f(x_1, x_2, \ldots, x_n) = \bigvee_{i=1}^{K} \bigwedge_{j \in P_i} x_j, \tag{6}$$

where n is the number of arguments of the function, K is the number of terms of the expression and the P_i are subsets of the interval $\{1, \ldots, N\}$. $\bigvee$ and $\bigwedge$ are Boolean operators AND and OR. It is possible to proof that this type of functions has the stacking property. If the function f used to filter an image X fulfills the stacking property, then from (4) and (5) it is deduced that, for two binary images X^i and X^j, obtained from X as the result of the application of the thresholds T^i and T^j respectively, the following implication is valid

$$i \geq j \Rightarrow X^i \leq X^j \Rightarrow f\left(X^i\right) \leq f\left(X^j\right) \tag{7}$$

A stack filter is defined by the function $S_f : \{0, \ldots, M\}^n \rightarrow \{0, \ldots, M\}$, corresponding to the Positive Boolean function $f(x_1, x_2, \ldots, x_n)$ expressed in the given form by (6). The function S_f can be expressed by means of

$$S_f(X) = \sum_{m=1}^{M} f\left(T^m(X)\right) \tag{8}$$

In Figure 1 it can be observed a scheme of aplication of the filter to an unidimensional signal. S_f represents the boolean function which filters each binary thresholded signal and whose outputs are added together to finally obtain the filtered signal.

3 Adaptive Algorithms for Stack Filters Design

In this work we applied the stack filter generated with the fast algorithm described in [21]. This algorithm arises as a result of studies on the methods proposed in [9]and [11]. To construct a stack filter following any of these methods, a training process that generates a positive boolean function that preserves the stacking property, represented by the so-called decision vector, is carried out. In what follows, the generation and behaviour of the decision vector

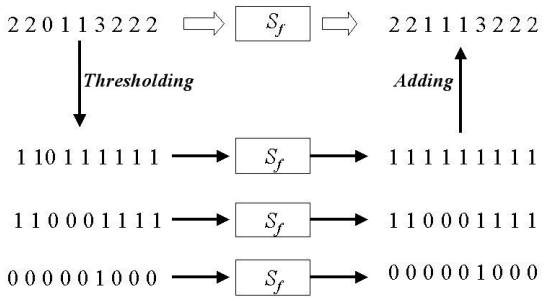

Figure 1. Scheme of the stack filter applied to an unidimensional signal. S_f represents the boolean function applied to each level.

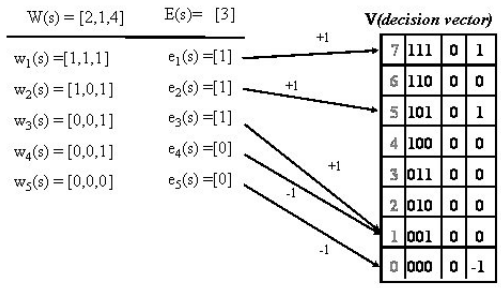

Figure 2. Scheme of the generation of the stack filter.

is explained. An image is defined as the set given by: $\{(s, v) : s \in S \subseteq \mathbb{Z}^2, v \in [0, \ldots, M], M \in \mathbb{Z}\}$, where s is position and v is the value of a pixel. Let E and R be two images, where R is the noisy version of E. A $W(s)$ window is a subimage of R of size $b = r \times r$ centered at position s. Let us define V as a 2^b dimension vector, and call it the decision vector. In the training phase of the filter design, for each $s \in S$, the data in $W(s)$ are decomposed in M thresholds obtaining M windows $w_i(s)$, $i = 1, \ldots, M$, where $w_i(s)$ is the ith thresholded version of $W(s)$. Then, for each $s \in S$ in the image E , a threshold $e_i(s)$ is defined (notice that here $e_i(s)$ has dimension 1). If $e_i(s) = 1$, then the position on V given by $w_i(s)$, considered as a binary number, is increased by one, if $e_i(s)$= 0, then the same position is decremented by 1. Periodically, V is checked to see wether the stacking property holds. If not, the decision vector V is suitably modified. Finally, the decision vector is transformed into a binary vector that is an implementation of the positive boolean function f sought. The training of this stack filter consists of the alternate application of two different stages: a stage in which the decision vector is modified according to the scheme indicated in Figure 2, and a stage in which the stacking property is checked and enforced on the decision vector.

4 SAR Images: the Multiplicative Model

In this section we introduce the statistical laws commonly used under the multiplicative model for Synthetic Aperture Radar (SAR) images. The multiplicative model considers the image returned by the SAR, named $\mathbf{Z}$, as a product of two independent random variables, one corresponding to the backscattter $\mathbf{X}$ and the other one corresponding to the speckle noise $\mathbf{Y}$, so

$$\mathbf{Z} = \mathbf{XY} \tag{9}$$

where we suppose independence among the random variables corresponding to each image pixel. We can write formula (9) for each pixel (i, j) of an image of size $M \times N$ as:

$$Z_{i,j} = X_{i,j}Y_{i,j},\ 0 \leq i \leq M-1,\ 0 \leq j \leq N-1. \tag{10}$$

The format of the SAR image (complex, amplitude or intensity) determines the distribution followed by the speckle noise random variables $Y_{i,j}$. These variables are i.i.d and the equivalent number of looks n is their only statistical parameter. On the other hand, the type of target each pixel belongs to (forest, pasture, crops, city) determines de most appropiate distribution for each of the backscatter random variables $X_{i,j}$. The speckle noise comes from the coherent addition of individual returns produced by elements present in each resolution cell. So, for example, in an image corresponding to a scene of land covered by vegetation, the returns from the elements of the plants and the ground are added taking into account the phase, yielding as a result a complex number. In an amplitude SAR image, the gray level of each pixel is the module of the this complex number. In an intensity SAR image, the gray level of each pixel is the square of this magnitude. For every pixel, the model for the speckle noise is the $\Gamma(n, 2n)$ distribution, where n is the equivalent number of looks. Then, within this model the density function for the speckle noise Y is given by

$$f_Y(y) = \frac{n^n}{\Gamma(n)} y^{n-1} e^{-ny},\ \ y \geq 0. \tag{11}$$

In SAR images the minimun for n is 1. This value corresponds to images generated without making the average of several looks. Images generated in this manner are noiser than those generated with more number of looks, but they have better azimuth resolution and, therefore, potencially

more information. We can suppose that the parameter n is known or that it can be estimated at an initial stage of the image analysis. Therefore, although in theory it would have to be an integer number, in practice it is necessary to consider it as a real number for the case in which it is estimated from the data. The moments of the speckle distribution are given by:

$$E[Y^r] = \frac{1}{n^r}\frac{\Gamma(n+r)}{\Gamma(n)} \tag{12}$$

where r is the moment order and $n \geq 1$ is the number of looks.

There are several models for the backscatter, that is, different statistical distributions exist for the random variables $X_{i,j}$. From the results presented in [7] it is possible to consider the Generalised Inverse Gaussian distribution as a general model for the backscatter. This distribution is very general and allows us to describe many different targets, but from an analitical and numerical point of view the estimation of its parameters is very complex and unstable. This distribution has various particular cases, one of which: the Inverse Gamma distribution, is of special interest to this work. This distribution is proposed as a universal model for SAR data and it leads to the $\mathcal{G}^0$ distribution for the return. The Inverse Gamma distribution, called Γ^{-1}, is characterised by the density function given by

$$f_X(x) = \frac{2^\alpha}{\gamma^\alpha \Gamma(-\alpha)} x^{\alpha-1} \exp\left(-\frac{\gamma}{2x}\right), \tag{13}$$

and its moments are expressed as

$$E\left[X^r\right] = \left(\frac{\gamma}{2}\right)^r \frac{\Gamma(-\alpha-r)}{\Gamma(-\alpha)}, \tag{14}$$

where $\alpha < 0$ and $|\alpha| > r$. The distribution corresponding to the return Z, is fixed by the distribution of the backscatter X and the distribution of the speckle Y. Given that $Z = XY$ and that these random variables are independent, $f_Z(z)$ can be calculated as

$$f_Z(z) = \int_{\mathbb{R}_+} f_{Z|Y=y}(z)\, f_Y(y)\, dy, \tag{15}$$

where $f_{Z|Y=y}$ is the density for the return Z considering $Y = y$ constant and f_Y the density function of the speckle Y. For the random variable corresponding to the return (intensity format) we have that $Z \sim \mathcal{G}^0(\alpha, \gamma, n)$, and the density function is given by

$$f_Z(z) = \frac{n^n \Gamma(n-\alpha)}{\left(\frac{\gamma}{2}\right)^\alpha \Gamma(-\alpha)\Gamma(n)} z^{n-1} \left(\frac{\gamma}{2} + nz\right)^{\alpha-n}, \tag{16}$$

with $\alpha < 0$, $\gamma > 0$ and $n \geq 1$. Given the independence between the backscatter X and the speckle Y, the moments of the return Z are the product of the moments of X and the moments of Y (equations (14) and (12)) yielding

$$\mathbb{E}\left[Z^r\right] = \left(\frac{\gamma}{2n}\right)^r \frac{\Gamma(-\alpha-r)}{\Gamma(-\alpha)} \frac{\Gamma(n+r)}{\Gamma(n)}, \tag{17}$$

recalling that these moments are finite for $-\alpha > r$. A statistical tool for characterizing the signal to noise ratio is the variation coefficient, defined as the ratio between the standard deviation and the mean value: C_V=σ/μ. The variation coeficient is given by

$$C_V = \frac{\sigma}{\mu} = -\frac{\sqrt{\alpha(\alpha+n+1)}}{\alpha}, \alpha < -(n+1),$$

where

$$\sigma^2 = \frac{\gamma^2}{4}\alpha(\alpha+n+1), \mu = \frac{-\alpha\gamma}{2}.$$

This distribution was proposed in [7] as a model for extremely heterogeneous data, but its utility for description of a great variety of natural and artificial targets was verified, which resulted in its being proposed as a universal model for SAR data.

5 Results

This section is dedicated to show the results of applying a stack filter to simulated and real SAR images. The simulated images are generated in such a way that their data have different degrees of homogeneity. We consider different values of the α and the γ parameters. The α parameter corresponds to image roughness (or heterogenity). It adopts negative values, varying from $-\infty$ to 0. If α is near 0, then the image data are extremely heterogeneous (for example: urban areas), and if α is far from the origin then the data correspond to a homogeneous region (for example: pasture areas), the values for forests and crops lay in-between. In order to evaluate the behaviour of the filters we carried out a maximun likelihood classification on real and synthetic images.

5.1 Statistical Analysis

An important task in statistical analysis is the characterization of the mean value and the variability of a data set. To this end, the behaviour of some statistics for filtered and non-filtered images, is compared. A set of images of $\mathcal{G}^0$ distributed data were generated using the values of α and γ. The α parameter varied between -1.5 and -8.5, and the γ parameter was adjusted so as to keep the mean value equal to one.

In order to design the stack filter, an image formed with

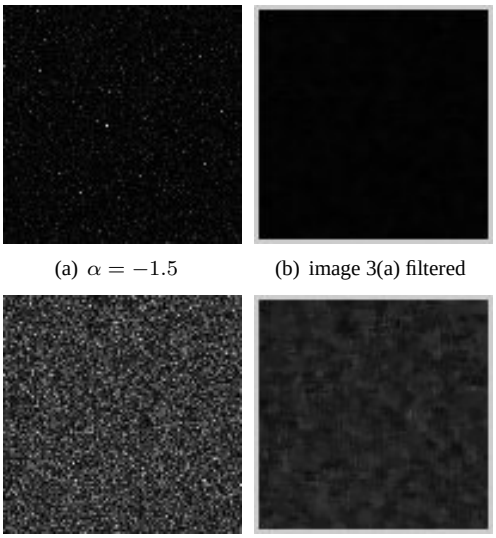

(a) $\alpha = -1.5$ (b) image 3(a) filtered

(c) $\alpha = -8.5$ (d) image 3(c) filtered

Figure 3. Simulated images and their corresponding filtered images.

the mean values of each region, as described in section 3, is used. Examples of these images are shown in Figure 3. This figure shows the results of applying an adaptive stack filter with a 3×3 window to images with different α values. Figures 3(a) and 3(c) correspond to the original speckled images and Figures 3(b) and 3(d) correspond to the filtered images.

It is observed that the value of C_V for the filtered images is lower than the value of C_V for the non-filtered images. This indicates that the effect of filtering is a decrease in the speckle noise. It is also observed that the value of C_V is lower when the α parameter is lower. For instance: for $\alpha = -1.5$ the values of C_V are 55.2 and 26.9 for the non-filtered and filtered images, respectively; for $\alpha = -8.5$ the values of C_V are 33.5 and 11.6 for the non-filtered and filtered images, respectively.

As γ is a scale parameter, the emphasis of this study is put only on the influence of the α parameter. The distribution of the data is modified when they are filtered. As a measure of asymmetry and peackedness we take into account the values obtained for skewness and kurtosis, respectively. The values obtained for these statistics indicate that filtered data are more Gaussian than non-filtered data. This improves the results obtained by maximum likelihood classification. Note that for a normal distribution the skewness is zero and the kurtosis is 3.

It can also be seen that for high values of α (heterogeneous data) the filtered data are less Gaussian than for lower values of α . This can be seen in Table 1, for $\alpha = -1.5$ and $\alpha = -8.5$.

Table 1. Kurtosis and Skewness

	Kurtosis		Skewness	
α	non filtered	filtered	non filtered	filtered
-1.5	81.58	1.05	5.79	0.54
-8.5	0.99	0.06	0.90	0.28

5.2 Maximum Likelihood Classification of Real and Simulated images

For this study, one hundred images, of size 128×128, were generated. These images had two regions: one simulating homogeneous data (for example, pasture) and the other simulating heterogeneous data (for example, city). The data in the first region followed a $\mathcal{G}^0(-8.5, 1, 1)$ distribution, and the data in the second region followed a $\mathcal{G}^0(-1.5, 1, 1)$ distribution. As an example, Figure 5(a) shows these two regions. Figure 5(b) shows the result of a Maximum Likelihood classification on the image of Figure 5(a), and Figure 5(c) and Figure 5(d) are the filtered and classified image, respectively.

From these images, the influence of stack filtering on Maximum Likelihood classification performance can be assessed. Table 2 shows the average confusion matrix where: R_i/R_j means the percentage of pixels that belong to region R_j but were classified into region R_i. From these values it can be seen that the classification performance was better for filtered images than for non- filtered images.

In order to test the proposed methodology on real SAR

Table 2. Average confusion matrix of a simulated images.

Image	R_1/R_1	R_2/R_1	R_2/R_2	R_1/R_2
non-filtered	70.76	29.24	88.49	11.51
filtered	**92.87**	7.13	**94.57**	5.43

data, a 256×256 1-look subimage was extracted. The adaptive algorithm was applied to a *ideal* image which consists of three regions with uniform values. Each of these values is computed as the mean value of the corresponding region in the original SAR image, see Figure 6(a) and Figure 6(b). Taking the original SAR image and the *ideal* image as inputs of the algorithm, the adaptive filter was generated. Then, this filter was applied ninety five times. At each iteration, the output image of the previous iteration was taken as the input image for the present one. Figures. 6(c) and 6(d) show the resulting images after 1 and 95 applications of the stack filter, respectively. Figure 7 shows the original image classified, and the classified

images corresponding to 1, 40 and 95 iterations. Figure 8 shows the images filtered by the Frost filter and the Lee filter, together with the corresponding classified images.

Table 3 shows the confusion matrices for the stack filter-based methods (1, 40 and 95 iterations), and for the Frost and the Lee filter-based methods. They are based on the training regions and the test regions depicted in Figure 4. These two filters were selected as a means of comparsion of the perfomance of the proposed methodology.

Data must be read as follows: R_i/R_j means the percentage of pixels that belong to region R_j but were classified into region R_i. From these values it can be seen that the classification performance was better for filtered images than for non-filtered images. It can also be seen that classificaton performance improves as the number of iterations is increased (see columns corresponding to $R_i/R_i,\ i = 1, 2, 3$).

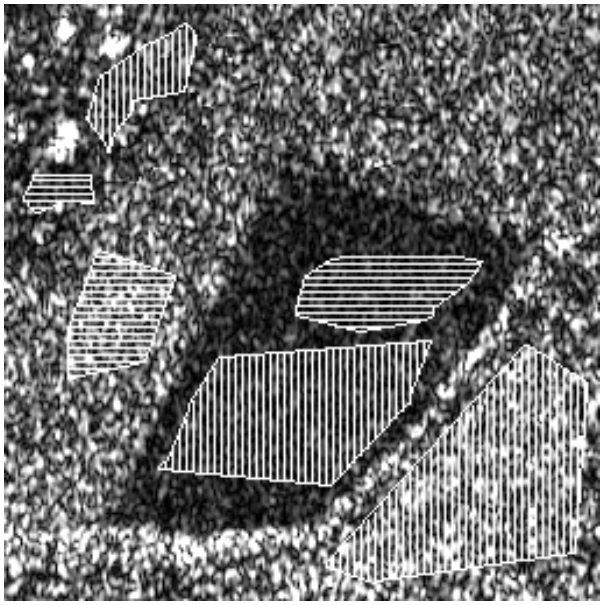

Figure 4. Training regions (horizontal lines fill) and test regions (vertical lines fill).

6 Conclusions

In this work, the effect of adaptive stack filtering of SAR images over classification accuracy was assessed. Synthetic and real images were used and the performance of repeatedly applying an adaptive stack filter was contrasted with the performance of Lee and Frost filtering. The preliminary

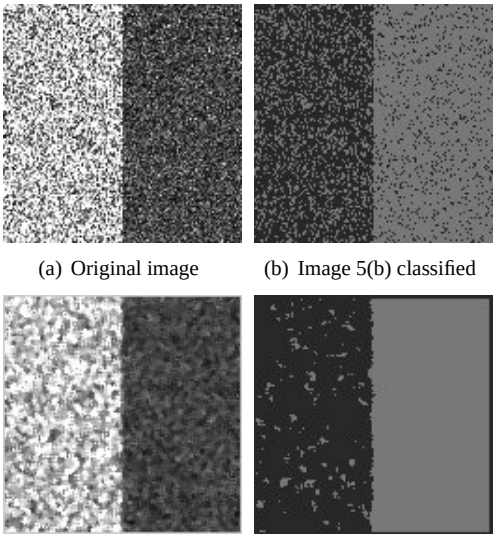

(a) Original image (b) Image 5(b) classified

(c) Filtered image (d) Image 5(d) classified

Figure 5. Synthetic, filtered and classified images

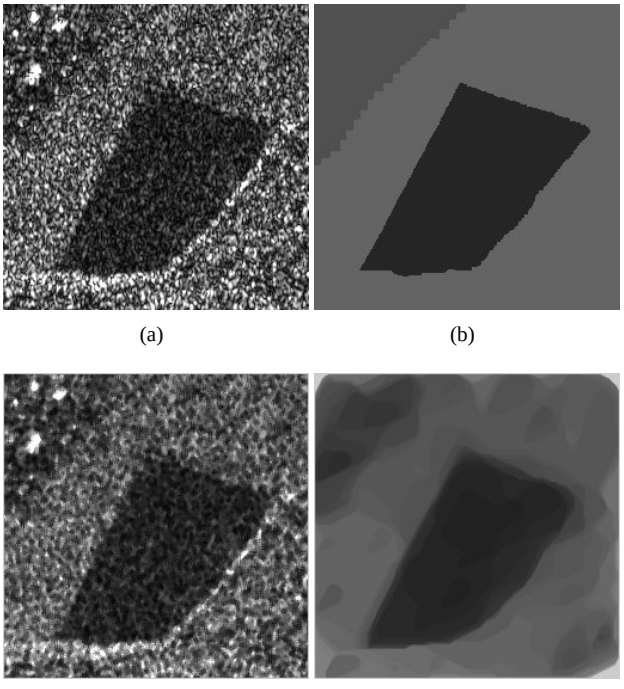

(a) (b)

(c) (d)

Figure 6. SAR filtered and classified images: a) orginal, b) ideal, c) filtered, one iteration, d) filtered, 95 iterations.

Table 3. Confusion matrix for real data.

Filter	R_1/R_1	R_2/R_1	R_3/R_1	R_1/R_2	R_2/R_2	R_2/R_3	R_1/R_3	R_2/R_3	R_3/R_3
Stack 1 it	14,35	36,10	49,55	12,82	64,65	22,53	5,32	3,82	90,86
Stack 40 it	62,81	22,42	14,77	10,40	89,09	0,51	4,65	1,24	94,11
Stack 95 it	**63,01**	25,03	11,96	6,43	**93,20**	0,37	4,26	1,70	**94,04**
FROST	16,55	31,02	52,43	17,71	55,54	26,74	6,36	3,47	90,17
LEE	16,38	30,70	52,93	17,24	52,72	30,04	7,19	3,60	89,21

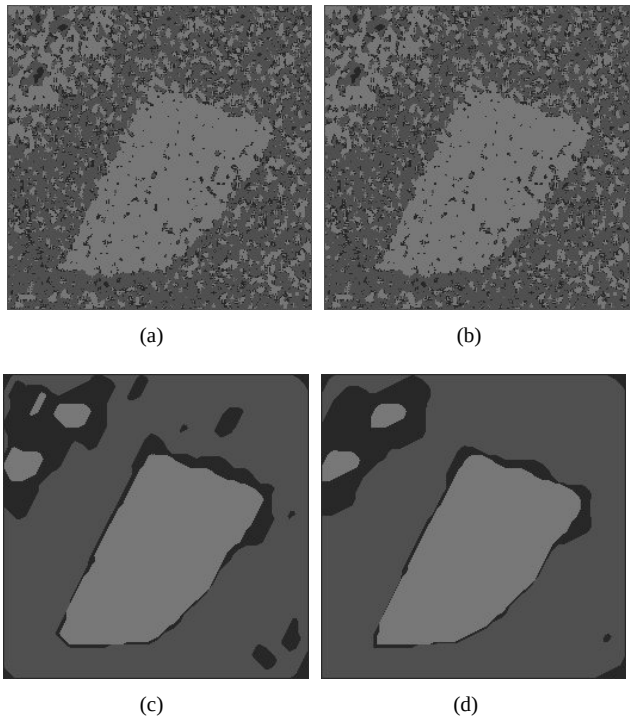

Figure 7. a) classified original, b) classified, one iteration, c) classified, 40 iterations and d) classified, 95 iterations.

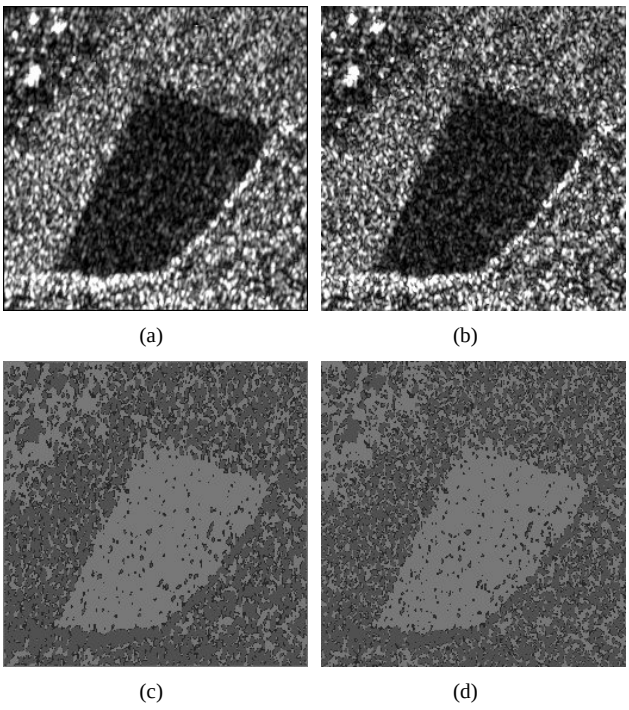

Figure 8. a) Frost filtered image , b) Lee filtered image , c) Frost filtered classified image , d) Lee filtered classified image.

results obtained show that, for the real image used for this study, consisting mainly of crop patches, the adaptive stack filter exhibited a better performance.

References

[1] J. Astola and P. Kuosmanen. *Fundamentals of Nonlinear Digital Filtering*. CRC Press, Boca Raton, 1997.

[2] E. J. Coyle, J.-H. Lin, and M. Gabbouj. Optimal stack filtering and the estimation and structural approaches to image processing. *IEEE Trans. Acoust., Speech, Signal Processing*, 37:2037–2066, 1989.

[3] J. Coyle and J.-H. Lin. Stack filters and the mean absolute error criterion. *IEEE Trans. Acoust., Speech, Signal Processing*, 36:1244–1254, 1988.

[4] D. Dellamonica, Jr., P. J. S. Silva, C. Humes, Jr., N. S. T. Hirata, and J. Barrera. An exact algorithm for optimal mae stack filter design. *Image Processing, IEEE Transactions on*, 16(2):453–462, Feb. 2007.

[5] D. Diaz and J. Paredes. Fpga implementation of a new family of stack filters. In *Devices, Circuits and Systems, 2004. Proceedings of the Fifth IEEE International Caracas Conference on*, volume 1, pages 152–157, 3-5 Nov. 2004.

[6] A. C. Frery, A. H. Correia, C. D. Rennó, C. C. Freitas, J. Jacobo-Berlles, M. E. Mejail, and K. L. P. Vasconcellos. Models for synthetic aperture radar image analysis. *Resenhas (IME-USP)*, 4(1):45–77, 1999.

[7] A. C. Frery, H.-J. Müller, C. C. F. Yanasse, and S. J. S. Sant'Anna. A model for extremely heterogeneous clutter. *IEEE Transactions on Geoscience and Remote Sensing*, 35(3):648–659, May 1996.

[8] J. W. Goodman. Some fundamental properties of speckle. *Journal of the Optical Society of America*, 66:1145–1150, 1976.

[9] H. J.Lin, T. M.Sellke, and E. J.Coyle. Adaptive stack filtering under the mean absolute error criterion. *IEEE Trans. Acoust., Speech, Signal Process*, 38:938–954, 1990.

[10] J.-S. Lee. Refined filtering of image noise using local statistics. 15(4):380–389, Apr. 1981.

[11] J.-H. Lin and Y. Kim. Fast algorithms for training stack filters. *IEEE Trans. Signal Processing*, 42(3):772–781, 4 1994.

[12] A. Lopes, E. Nezry, R. Touzi, and H. Laur. Structure detection and statistical adaptive speckle filtering in SAR images. *International Journal of Remote Sensing*, 14(9):1735–1758, 1993.

[13] M. E. Mejail, J. Jacobo-Berlles, A. C. Frery, and O. H. Bustos. Classification of SAR images using a general and tractable multiplicative model. *International Journal of Remote Sensing*, 24(18):3565–3582, 2003.

[14] C. Oliver and S. Quegan. *Understanding synthetic aperture radar images*. Artech House, 1998.

[15] J. Paredes and G. Arce. Stack filters, stack smoothers, and mirrored threshold decomposition. *Signal Processing, IEEE Transactions on [see also Acoustics, Speech, and Signal Processing, IEEE Transactions on]*, 47(10):2757–2767, Oct. 1999.

[16] M. Prasad. Stack filter design using selection probabilities. *Signal Processing, IEEE Transactions on [see also Acoustics, Speech, and Signal Processing, IEEE Transactions on]*, 53(3):1025–1037, Mar 2005.

[17] G. Shi, W. Dong, and Z. Liu. Design and implementation of stack filter based on immune memory clonal algorithms with hybrid computation. In *Circuits and Systems, 2005. 48th Midwest Symposium on*, pages 1159–1162Vol.2, 7-10 Aug. 2005.

[18] D. Smith. Speckle Reduction and Segmentation of SAR Images. *International Journal of Remote Sensing*, 17(11):2043–205, 199.

[19] K. S. J. H. V.S. Frost, J.A. Stiles. A model for radar images and its application to adaptive digital filtering of multiplicative noise. *IEEE Transactions on Pattern Analysis and Machine Intelligence*, 4:157–166, mar 1982.

[20] P. Wendt, E. J. Coyle, and J. N.C. Gallangher. Stack filters. *IEEE Trans. Acoust. Speech Signal Processing*, 34:898–911, 8 1986.

[21] J. Yoo, K. L. Fong, J.-J. Huang, E. J. Coyle, and G. B. A. III. A fast algorithm for designing stack filters. *IEEE Trans.on image processing*, 8(8):772–781, 8 1999.